

Genome-wide association and interaction studies of CSF T-tau/A β ₄₂ ratio in ADNI cohort

Jin Li^a, Qiushi Zhang^{a,b}, Feng Chen^a, Xianglian Meng^a, Wenjie Liu^a, Dandan Chen^{a,b}, Jingwen Yan^{c,d,e}, Sungeun Kim^c, Lei Wang^a, Weixing Feng^a, Andrew J. Saykin^c, Hong Liang^{a,*}, Li Shen^{c,d,e,*}, and for the Alzheimer's Disease Neuroimaging Initiative^{**}

^aCollege of Automation, Harbin Engineering University, 145 Nantong Street, Harbin, China, 150001

^bCollege of Information Engineering, Northeast Dianli University, 169 Changchun Street, Jilin, China, 132012

^cCenter for Neuroimaging, Department of Radiology and Imaging Sciences, Indiana University School of Medicine, 355 West 16th Street, Suite 4100, Indianapolis, IN 46202

^dCenter for Computational Biology and Bioinformatics, Indiana University School of Medicine, 410 West 10th Street, Suite 5000, Indianapolis, IN 46202

^eDepartment of BioHealth Informatics, Indiana University School of Informatics and Computing, Indianapolis, IN 46202

Abstract—The pathogenic relevance in Alzheimer's disease (AD) presents a decrease of cerebrospinal fluid (CSF) amyloid- β ₄₂ (A β ₄₂) burden and an increase in CSF total-tau (T-tau) levels. In this work, we performed genome-wide association study (GWAS) and genome-wide interaction study (GWIS) of T-tau/A β ₄₂ ratio as an AD imaging quantitative trait (QT) on 843 subjects and 563,980 single nucleotide polymorphisms (SNPs) in ADNI cohort. We aim to identify not only SNPs with significant main effects but also SNPs with interaction effects to help explain "missing heritability". Linear regression method was used to detect SNP-SNP interactions among SNPs with uncorrected p-value ≤ 0.01 from the GWAS. Age, gender and diagnosis were considered as covariates in both studies. The GWAS results replicated the previously reported AD-related genes *APOE*, *APOC1* and *TOMM40*, as well as identified 14 novel genes, which showed genome-wide statistical significance. GWIS revealed 7 pairs of SNPs meeting the cell-size criteria and with bonferroni-corrected p-value ≤ 0.05 . As we expect, these interaction pairs all had marginal main effects but explained a relatively high-level variance of T-tau/A β ₄₂, demonstrating their potential association with AD pathology.

Keywords: Cerebrospinal fluid (CSF), Amyloid- β ₄₂ (A β ₄₂), Total tau (T-tau), T-tau/A β ₄₂ ratio, GWIS, ADNI.

1. Introduction

Alzheimer's disease (AD) is the most common form of dementia and characterized by pathological results at autopsy of the accumulation of amyloid- β (A β) protein in senile plaques and hyper-phosphorylated tau in neurofibrillary tangles in brain (Mukaetova-Ladinska et al., 2015). The levels of two measures, cerebrospinal fluid (CSF) amyloid- β ₄₂ (A β ₄₂) and total tau (T-tau), have been shown strong promise as predictive biomarkers of the progression from mild cognitive impairment (MCI, a prodromal stage of AD) to AD (Blennow and Hampel, 2003; Pan et al., 2015). Typically, the pathogenic relevance in AD presents a decrease of CSF A β ₄₂ burden and an increase in CSF T-tau levels simultaneously (Li et al., 2015).

However, the emerging literatures reported that a group of individuals have never shown clinical symptoms of AD in their

lifetime but detected out tauopathies and amyloid plaques at autopsy (Hohman et al., 2014). In addition, some normal cognitive individuals presented low CSF A β ₄₂ burden and some individuals with definitive diagnosis of AD showed high levels of CSF A β ₄₂ due to their lack of amyloid deposition (Fagan et al., 2006). The emergence of this situation posed challenges on discriminating individuals with AD from normal cognitive, and affected the diagnostic potential of these markers. To address this issue, a potential biomarker CSF T-tau/A β ₄₂ ratio demonstrated its predictive ability. It can be used to detect and measure the AD risk with cognitive decline in non-demented older adults, and individuals with higher ratio tend to have higher risk to develop AD (Fagan et al., 2007). Moreover, prior studies also showed that individuals with family history of AD had higher risk for AD than those without a family history. This indicates that the underlying genetic factors may play an important role in AD (Hohman et al., 2014).

The existing genome-wide association studies (GWAS) have analyzed Single Nucleotide Polymorphism (SNP) data and discovered a wide array of underlying genetic causes of AD and genetic associations with AD biomarkers as intermediate quantitative traits (QTs). For many conditions of complex diseases and traits, commonly used single marker analysis can identify a number of risk genetic loci, but these identified variants typically appear to explain only a modest portion of the theoretical estimates of genetic heritability (Goudey et al., 2013). One possible reason is that the univariate methods used in GWAS typically ignore the factor of underlying genetic interaction, which may contribute to the development of disease and trait variance.

* Corresponding author at:

College of Automation, Harbin Engineering University, 145 Nantong Street, 150000, Harbin, China. Tel.: +86 137 9667 9740.

E-mail address: lh@hrbeu.edu.cn (Hong Liang).

Center for Neuroimaging, Department of Radiology and Imaging Sciences, Indiana University School of Medicine, 355 West 16th Street, Suite 4100, IN 46202 Indianapolis, USA. Tel.: 317 963-7504; fax: 317 963-7504

E-mail address: shenli@iu.edu (Li Shen).

** Data used in preparation of this article were obtained from the Alzheimer's Disease Neuroimaging Initiative (ADNI) database (adni.loni.usc.edu). As such, the investigators within the ADNI contributed to the design and implementation of ADNI and/or provided data but did not participate in analysis or writing of this report. A complete listing of ADNI investigators can be found at: http://adni.loni.usc.edu/wp-content/uploads/how_to_apply/ADNI_Acknowledgement_List.pdf.

This is the author's manuscript of the article published in final edited form as:

Li, J., Zhang, Q., Chen, F., Meng, X., Liu, W., Chen, D., ... Shen, L. (2017). Genome-wide association and interaction studies of CSF T-tau/A β ₄₂ ratio in ADNI cohort. *Neurobiology of Aging*.

<https://doi.org/10.1016/j.neurobiolaging.2017.05.007>

Thus, one of several putative explanations for the “missing heritability” is that the trait variance can partially be explained by the SNP-SNP interaction effects in addition to their main effects (Becker et al., 2011). Therefore, genome-wide interaction studies (GWIS) have recently gained substantial attention (J. Li et al., 2015).

In this study, we performed both GWAS and GWIS in the Alzheimer’s Disease Neuroimaging Initiative (ADNI) cohort. We used the AD-associated CSF T-tau/A β_{42} ratio as QT, and tested single-marker main effects and two-marker interactions at the genome-wide level.

2. Materials and Methods

Data used in the preparation of this article were obtained from the Alzheimer’s Disease Neuroimaging Initiative (ADNI) database (adni.loni.usc.edu). The ADNI was launched in 2003 as a public-private partnership, led by Principal Investigator Michael W. Weiner, MD. The primary goal of ADNI has been to test whether serial magnetic resonance imaging (MRI), positron emission tomography (PET), other biological markers, and clinical and neuropsychological assessment can be combined to measure the progression of mild cognitive impairment (MCI) and early Alzheimer’s disease (AD).

We applied for and were granted permission to use data from the ADNI cohort (<http://www.adni-info.org/>) to conduct genetic association and interaction analyses.

2.1. Subjects

Participants are ADNI subjects (N=843) with CSF T-tau and A β_{42} measures and quality controlled genotyping data available at baseline. The sample included 199 cognitively normal (CN), 85 significant memory concern (SMC), 239 early mild cognitive impairment (EMCI), 207 late mild cognitive impairment (LMCI), and 113 AD participants. Table 1 shows selected participant characteristics at the baseline, which is the time point studied in this work.

2.2. Quality control of genotyping data

The genotyping data of the ADNI-1, ADNI-GO and ADNI-2 cohorts were collected using either the Illumina 2.5M array (a byproduct of the ADNI whole genome sequencing sample) or

the Illumina OmniQuad array (Saykin et al., 2010; Shen et al., 2010; Shen et al., 2014), and were downloaded from the LONI website (<http://adni.loni.usc.edu>). For the present analyses, we included SNPs that were present on both arrays.

Quality control (QC) was performed using the PLINK software (version 1.90) (Purcell et al., 2007). SNPs were removed from the analysis if any of the following criteria were not satisfied: (1) SNPs on chromosome 1-22; (2) call rate per SNP $\geq 95\%$; (3) minor allele frequency $\geq 5\%$ (1,845,510 SNPs were removed based on Criteria 1, 2 and 3); and (4) Hardy-Weinberg equilibrium (HWE) test of $p \geq 10^{-6}$ using CN subjects only (198 SNPs were removed). Participants not meeting any of the following criteria were removed from further analyses: (1) call rate per participant $\geq 90\%$ (none); (2) sex check (1 participant was removed); and (3) identity check for related pairs (8 sibling pairs and one triplet were identified with PI_HAT ≥ 0.25 , 9 participants (one from each pair or triplet) were randomly selected and included in this study).

Population stratification analysis was performed using EIGENSTRAT (Price et al., 2006), and confirmed using STRUCTURE (Pritchard et al., 2000). It yielded 89 participants who did not cluster with the remaining subjects and with the CEU HapMap samples who are primarily of European ancestry (non-Hispanic Caucasians). These 89 participants were excluded from the analysis. Among the remaining 1,079 subjects, only 843 subjects have both genotyping data and phenotypes (T-tau and A β_{42}) after quality control (QC), and thus the other 236 participants were excluded.

After QC, 843 subjects and 563,980 SNPs remained for the subsequent genome-wide association and interaction analyses.

2.3. CSF T-tau/A β_{42} biomarker

In our study, the CSF levels of T-tau and A β_{42} at baseline were used. The methods for CSF acquisition and biomarker measurement have been reported previously (Hampel et al., 2010; Jagust et al., 2009; Shaw et al., 2009). For this analyses, the A β_{42} and T-tau data were log-transformed to better approximate normality in distribution (Dickerson et al., 2013), and the values greater or smaller than 4 SDs (standard deviation) from the mean value of A β_{42} and T-tau were regarded as extreme outliers and excluded from the analyses.

Table 1. The demographic and clinical characteristics of 843 ADNI participants at baseline studied in this work.

	CN (N=199)	SMC (N=85)	EMCI (N=239)	LMCI (N=207)	AD (N=113)
Age (years)	74.4(7.79)	72.0(5.48)	71.4(7.30)	72.4(7.61)	75.2(8.19)
Women	96(48.2%)	50(58.8%)	102(43.6%)	83(40.1%)	45(39.8%)
Education (years)	16.21(2.82)	16.00(2.79)	16.16(2.80)	16.38(2.53)	16.40(2.56)
APOE e4 allele present	47(23.6%)	31(36.5%)	99(41.4%)	112(54.1%)	74(65.5%)
CDR-SOB	0.04(0.14)	0.08(0.18)	1.27(0.77)	1.65(0.94)	4.53(1.70)
Mini mental status examination	29.06(1.18)	29.04(1.420)	28.34(1.62)	27.54(1.75)	23.12(2.04)
Logical memory immediate recall (WMS-R)	14.42(3.00)	14.44(3.34)	11.09(2.68)	7.18(3.06)	4.15(2.70)
Logical memory delayed recall (WMS-R)	13.34(3.12)	13.29(3.31)	8.97(1.73)	3.94(2.70)	1.52(1.80)
CSF T-tau (Total tau)	69.76(31.76)	66.95(31.68)	77.66(46.97)	98.22(52.50)	126.26(54.47)
CSF A β_{42} (amyloid- β_{42})	198.09(52.87)	201.42(49.43)	184.50(51.41)	162.92(52.80)	136.90(36.25)
Quantitative Traits (QTs)	T-tau/A β_{42} ratio				
	0.40(0.27)	0.37(0.24)	0.50(0.45)	0.70(0.47)	0.98(0.49)

Abbreviations: AD, Alzheimer’s disease; ADNI, Alzheimer’s Disease Neuroimaging Initiative; CDR-SOB, clinical dementia rating-sum of boxes; CN, cognitively normal; SMC, significant memory concern; EMCI, early mild cognitive impairment; LMCI, late mild cognitive impairment; WMS-R, Wechsler Memory Scale-Revised. Data are number (%) or mean (s.d.).

After QC, 843 valid CSF samples remained.

2.4. Method of GWAS and GWIS

GWAS was used to evaluate the SNPs main effects at the genome-wide level. Our study performed a genotypic model based GWAS using PLINK 1.90 to detect the association between SNPs and the T-tau/AB₄₂ ratio with age, gender and clinical diagnosis (five values (1-5) indicating CN, SMC, EMCI, LMCI and AD respectively) as covariates. Manhattan plots and quantile-quantile (Q-Q) plots were generated using Haploview (<http://www.broad.mit.edu/mpg/haploview/>) and R (<http://www.r-project.org>) respectively.

For GWIS detecting the SNP-SNP interactions, software tool INTERSNP (Herold et al., 2009) was used for two-marker analysis. The input files of the tool were PLINK genotype files. Firstly, single-marker test was performed for GWAS as previously described. The SNPs that met the threshold (uncorrected p-value ≤ 0.01) were included in the subsequent interaction analysis. Linear regression model was used for an additive interaction test (full model including both additive and dominance effects plus interaction term versus reduced model that does not contain interaction terms) on all possible SNP pairs among the previous SNPs selected in first step. We detected the epistasis interactions with the T-tau/AB₄₂ ratio as QT while controlling for covariates including the baseline age, gender, and clinical diagnosis. There were about 22 million unique SNP pairs to be examined, and the Bonferroni corrected p-value < 0.05 was used as the statistical significance threshold.

2.5. Post hoc analysis

We performed a hierarchical linear regression among the significant interactions, used IBM SPSS 20 to estimate the amount of variance (R^2) on the T-tau/AB₄₂ level accounted for by these interaction terms. We first included the same set of covariates (age, gender, and diagnosis) in the linear model, and then included apolipoprotein E (APOE) status, the best-known AD risk gene (Akiyama et al., 1993), and two main effects of SNPs from the significant pair. Finally, we included the SNP-SNP interaction term and computed additional variance explained by interaction term. The difference in R^2 for the

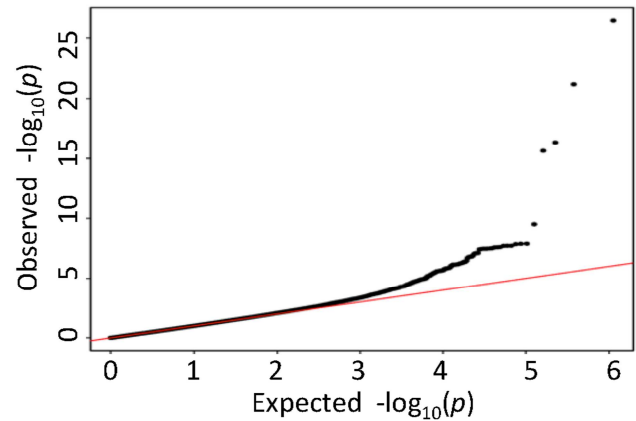


Fig. 1. Quantile-quantile (Q-Q) plot of the observed $-\log_{10}(p)$ -values from the GWAS of T-tau/AB₄₂ level versus those expected under the null hypothesis.

significant model was calculated in SPSS as $\Delta R^2 = R^2_{\text{full}} - R^2_{\text{domain}}$ (full model with interaction term) – R^2_{domain} (reduced model without interaction term).

3. Results

3.1. Genome-wide association study results

The demographic and clinical characteristics of the 843 participants at baseline were shown in Table 1. Q-Q plot (Fig. 1) shows five evident outliers at the high end of the range, and indicates no evidence of spurious inflation. The Manhattan plot in Fig. 2 shows the same five outliers with high significance, and there are a few other significant hits shown above the red line (Bonferroni-corrected threshold p-value = 0.05).

In single-marker analyses, 24 SNPs exhibited genome-wide significance to the T-tau/AB₄₂ ratio (Table 2). As expected, the most significant loci were identified on chromosome 19, including rs4420638 ($p=3.50E-27$) from the *APOC1* region, rs769449 ($p=6.41E-22$) within the *APOE* region, and rs2075650 ($p=4.40E-17$) and rs157582 ($p=2.29E-16$) within the *TOMM40* region. Other SNPs identified in this study are shown in Table 2. Table 2 also shows the variances explained by each identified SNP after controlling two sets of covariates: (1) age, gender, and diagnosis; and (2) age, gender, diagnosis,

Table 2. Identified significant genome-wide association loci with quantitative trait T-tau/AB₄₂ in this study.

NO.	CHR	rs_No.	Gene	Single-marker p-value	Corrected p-value	R Square		No.	CHR	rs_No.	Gene	Single-Marker p-Value	Corrected p-value	R Square	
						Model ^a	Model ^b							Model ^a	Model ^b
1	19	rs4420638	<i>APOC1</i>	3.50E-27	1.97E-21	0.100	0.001	13	1	rs10127852	<i>LPAR3</i>	2.46E-08	0.0137	0.034	0.023
2	19	rs769449	<i>APOE</i>	6.41E-22	3.62E-16	0.091	0.0	14	15	rs9806191	<i>DAPK2</i>	2.56E-08	0.0143	0.034	0.023
3	19	rs2075650	<i>TOMM40</i>	4.40E-17	2.48E-11	0.071	0.0	15	11	rs7129826	<i>DBX1</i>	2.99E-08	0.0167	0.033	0.023
4	19	rs157582	<i>TOMM40</i>	2.29E-16	1.25E-10	0.068	0.001	16	21	rs11910985	<i>SI00B</i>	3.17E-08	0.0177	0.033	0.023
5	1	rs13376197	<i>B3GALT2</i>	3.04E-10	0.00017	0.042	0.031	17	21	rs1981331	<i>SI00B</i>	3.19E-08	0.0178	0.033	0.023
6	12	rs3020811	<i>LRP6</i>	1.24E-08	0.0069	0.030	0.026	18	3	rs9872004	<i>AADACL1</i>	3.26E-08	0.0181	0.033	0.023
7	9	rs2280302	<i>FBP1</i>	1.28E-08	0.0071	0.035	0.026	19	1	rs17027633	<i>ATP5F1</i>	3.26E-08	0.0182	0.033	0.023
8	9	rs2280301	<i>FBP1</i>	1.37E-08	0.0076	0.035	0.026	20	1	rs6662771	<i>SGIP1</i>	3.44E-08	0.0192	0.033	0.023
9	10	rs12265790	<i>ITGA8</i>	1.85E-08	0.0103	0.034	0.024	21	11	rs12797204	<i>DLG2</i>	3.71E-08	0.0206	0.033	0.025
10	10	rs7896076	<i>ITGA8</i>	1.87E-08	0.0104	0.034	0.024	22	18	rs6506440	<i>ARHGAP28</i>	7.51E-08	0.0414	0.032	0.026
11	10	rs11253637	<i>ITGA8</i>	1.91E-08	0.0107	0.034	0.024	23	2	rs6541929	<i>CNTNAP5</i>	7.64E-08	0.0421	0.032	0.027
12	1	rs1539581	<i>ATP5F1</i>	2.34E-08	0.0130	0.034	0.024	24	2	rs17267326	<i>CNTNAP5</i>	8.23E-08	0.0453	0.031	0.028

^a Model: Percent of additional variance in T-tau/AB₄₂ level explained by the main effect of SNPs after accounting for age, gender, and diagnosis.

^b Model: Percent of additional variance in T-tau/AB₄₂ level explained by the main effect of SNPs after accounting for age, gender, diagnosis, and the *APOE*

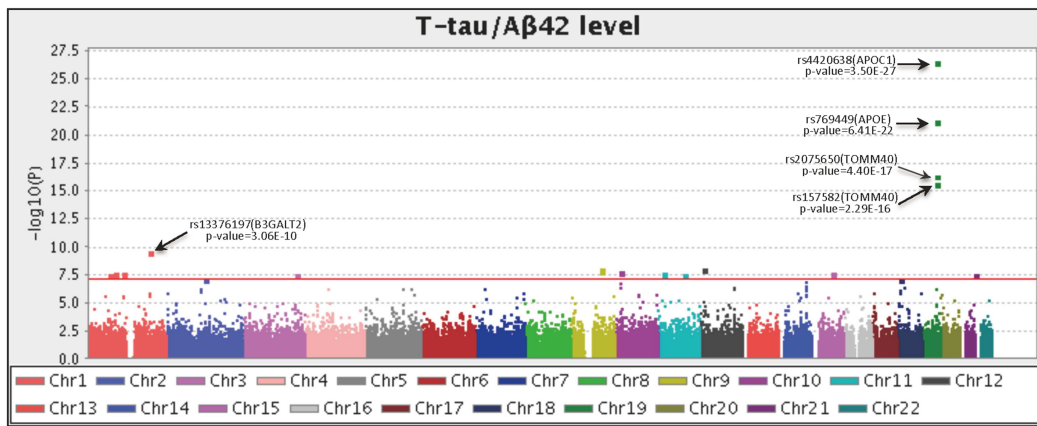


Fig. 2. Manhattan plot of the observed $-\log_{10}(p\text{-values})$ from the GWAS CSF. More than 560,000 SNPs were tested for association to T-tau/A β_{42} level under an genotypic model with age, gender and diagnosis as covariates. Genome-wide associations identified 22 significant SNPs (Bonferroni-corrected threshold is $p\text{-value} < 0.05$ and represented by the red line), and the top 4 significant SNPs were on chromosome 19 within the *APOE* and its neighboring regions.

and the *APOE* $\epsilon 4$ status. The main effects of rs4420638, rs769449, rs2075650, and rs157582 account for 10%, 9.1%, 7.1%, and 6.8% of phenotypic variance respectively while controlling for age, gender and diagnosis, but account for $\leq 0.1\%$ variance after removing the *APOE* $\epsilon 4$ status. The most significant AD-risk factor *APOE* $\epsilon 4$ SNP (rs429358) accounts for 12.9% variance (Table 3). The total amount of additional variance explained by 24 identified SNPs is 11.3% after accounting for age, gender, diagnosis and *APOE* $\epsilon 4$ status, and up to 41.6% while including all factors (age, gender, diagnosis, *APOE* and 24 SNPs).

3.2. Genome-wide interaction study results

Our two-marker interaction model considered age, gender, and clinical diagnosis as covariates. 307 pairs of SNPs showed statistically significant interaction effects on the T-tau/A β_{42} level (Bonferroni-corrected $p\text{-value} < 0.05$). Only 7 pairs passed the cell-size criterion: all the cell sizes in 3-by-3 contingency table are required to be either more than 5 or equal to 0. The results of two-marker interaction were: rs1514061 (*PLXNA4**) - rs6467419 (*PLXNA4**), rs1514061 (*PLXNA4**) - rs4453471 (*CDH13*), rs7303599 (*ADIPOR2**) - rs7146454 (*ADSSLI**), rs7303599 (*ADIPOR2**) - rs167396 (*GSN**), rs1482548 (*INHBA**) - rs12894119 (*NIN**), rs9550406 (*MTUS2**) - rs6471951 (*RLBP1L*), rs211953 (*CXADR*) - rs4881147 (*PITRM1**), where * indicating nearest gene proximal to the SNP. Details are available in Table 3.

3.3. Post hoc analysis

Table 3 also shows the two-marker interaction results of post hoc analysis on T-tau/A β_{42} level. Age, gender, and diagnosis were first included in the model and accounted for 17.4% of variance on the T-tau/A β_{42} level. *APOE* status was then accounted for an additional 12.9% of variance. For each interaction, we ran a hierarchical linear regression model. We first added in the genetic main effects, and then the genetic interaction term to determine the variance associated with the interaction term alone. For rs1514061 (*PLXNA4**) - rs6467419 (*PLXNA4**), the SNPs' main effects accounted for 1.5% of variance, and the interaction term accounted for 5.1% of variance (6.6% combined). For rs1514061 (*PLXNA4**) - rs4453471 (*CDH13*), the main effects accounted for 1.9% of

variance, and the interaction accounted for 4.7% of variance (6.6% combined). For rs7303599 (*ADIPOR2**) - rs7146454 (*ADSSLI**), the main effects accounted for 2.3% of variance, and the interaction term accounted for 4.2% of variance (6.5% combined). For rs7303599 (*ADIPOR2**) - rs167396 (*GSN**), the main effects accounted for 2.1% of variance, and the interaction term accounted for 4.1% of variance (6.2% combined). For rs1482548 (*INHBA**) - rs12894119 (*NIN**), the main effects accounted for 1.5% of variance, and the interaction term accounted for 3.8% of variance (5.3% combined). For rs9550406 (*MTUS2**) - rs6471951 (*RLBP1L*), the main effects accounted for 1.0% of variance, and the interaction accounted for 3.4% of variance (4.4% combined). For rs211953 (*CXADR*) - rs4881147 (*PITRM1**), the main effects accounted for 2.4% of variance, and the interaction term accounted for 3.1% of variance (5.5% combined).

4. Discussion

In this work, we performed GWAS and GWIS of the CSF biomarker T-tau/A β_{42} ratio, using a sample of 843 subjects from the ADNI database. To our knowledge, this genome-wide study on detecting two-marker interaction is the first GWIS on the quantitative trait of the T-tau/A β_{42} level.

In single-marker analysis, we identified the SNPs in *APOE*, *APOC1* and *TOMM40* genes (Fig. 2), which showed high-level genome-wide significant associations to the T-tau/A β_{42} ratio. We also revealed 20 additional significant loci, within or proximal to *LRP6*, *S100B*, *DLG2*, *CNTNAP5*, *B3GALT2*, *FBP1*, *ITGA8*, *ATP5F1*, *LPAR3*, *DAPK2*, *DBX1*, *AADACL1*, *SGIP1*, and *ARHGAP28* genes (Table 2). The previously reported AD risk genes *APOE*, *APOC1*, and *TOMM40* were replicated in our GWAS (Supplementary Table s4). In addition, the *S100B*, *CNTNAP5*, *LRP6*, and *DLG2* genes were also reported to have pathological relevances in AD. *S100B* shows a pathological relevance for degeneration of the central nervous system in AD (Petzold et al., 2003), and overexpression of *S100B* in the neuritic plaques of AD is related to the degree of neuritic pathology in A β plaques (Peskind et al., 2001). *CNTNAP5* encodes the protein belonging to the neuroligin family functioning in the central nervous system as cell

adhesion molecules and receptors, and has been implicated as a risk factor for posterior cortical atrophy variant of AD (Schott et al., 2016). Neuronal *LRP6* mediated Wnt signaling has an impact on synaptic function and cognition, and genetic variants in the *LRP6* gene have been linked to AD risk (Liu et al., 2014). A proteomics study showed AD-dependent changes in the DLG2 level in the hippocampus, and DLG2 exhibits an early-up, late-down expression pattern during AD pathology (Hondius et al., 2016). Our exploratory GWAS nominates the others novel loci, such as *B3GALT2*, *FBP1*, *ITGA8*, *ATP5F1*, *LPAR3*, *DAPK2*, *DBX1*, *AADACL1*, *SGIP1* and *ARHGAP28*, meeting the genome-wide significance. These potential T-tau/A β ₄₂ related quantitative trait loci (QTLs) warrant further investigation.

SNP-SNP interaction studies may explain part of the “missing heritability”. The recent studies (Shen et al., 2014) in ADNI cohort demonstrated “case-control” studies for testing epistasis interaction. In this study, we preformed two-marker interaction analyses using the T-tau/A β ₄₂ ratio as quantitative trait for increasing statistical power and reducing required sample sizes. Our method revealed 7 pairs of SNPs within or proximal to 11 genes meeting the criterion of the cell size either more than 5 or equal to 0 and a Bonferroni corrected threshold (corrected p-value ≤ 0.05). As we expected, the significant variants in these pairs all have marginal dominance effects, but their interactions can explain a relatively high-level variances of the T-tau/A β ₄₂ ratio (Table 3), and high-level AD risk. The bar charts of the QT measures across SNP-by-SNP genotype combinations are shown in Fig. 3.

In previous studies, *PLXNA4* has been reported to be associated with precise positioning of OPCs (oligodendrocyte precursor cells) in developing cerebral cortex. Then it has also suggested that *PLXNA4* does not influence APP processing or A β production but its isoform differentially affects tau protein phosphorylation (Jun et al., 2014) involved in AD pathogenesis, leading to neurofibrillary tangle formation and neuronal death (Wang et al., 2016). *CDH13* gene has been linked to brain function or neuropsychiatric disorders, affecting morphometry of the temporal lobes (a typical AD biomarker) (Kohannim et al., 2012). With these observations, the identified *PLXNA4-PLXNA4* and *PLXNA4-CDH13* interactions may have a potential on contributing to the tau pathway instead of A β .

ADIPOR2 (Adiponectin Receptor 2) is a protein coding gene, and adiponectin is the most abundant adipokine secreted from adipose tissue. Globular adiponectin has been reported to induce a pro-inflammatory response in human astrocytic cells (Chan et al., 2012; Wan et al., 2014). A β caused neuroinflammation plays a critical role in the development of neurodegenerative disorder in AD pathogenesis. *ADSSL1* is an A β toxicity modifier gene, and also an intracellular protein responsible for catalyzing the first step of de novo biosynthesis of AMP. Its genetic variation has been shown to affect AD neuropathology and episodic memory (Rosenthal et al., 2012). *GSN* (Gelsolin) is a protein coding gene, and Gelsolin is one of the most abundant actin-binding proteins. Gelsolin binds to A β protein, inhibits its fibrillization, solubilizes preformed A β fibrils, and helps in its clearance from the brain (Yang et al., 2014). It is involved in several pathological processes, including AD (Deng et al., 2015). With these observations, the identified *ADIPOR2-ADSSL1* and *ADIPOR2-GSN* interactions could be related to the A β pathway.

Table 3. Seven significant SNP-SNP interaction pairs identified in the GWIS of the T-tau/A β ₄₂ ratio.

NO.	SNP1×SNP2	GENE	CHR	Main Effect	Interaction		Explained Variance (R Square)				
				p-value	p-value	Corrected p-value	Age+Gender ^a	Dx ^b	APOE ^c	SNP1+SNP2 ^d	SNP1*SNP2 ^e
1	rs1514061×	PLXNA4*	7	3.41E-06	8.35E-10	0.0181	0.01	0.164	0.129	0.015	0.051
	rs6467419	PLXNA4*	7	0.00167353							
2	rs1514061×	PLXNA4*	7	3.41E-06	1.97E-10	0.0043	0.01	0.164	0.129	0.019	0.047
	rs4453471	CDH13	16	0.00377003							
3	rs7303599×	ADIPOR2*	12	7.91E-05	5.76E-11	0.0013	0.01	0.164	0.129	0.023	0.042
	rs7146454	ADSSL1*	14	0.00733134							
4	rs7303599×	ADIPOR2*	12	7.91E-05	6.91E-10	0.0150	0.01	0.164	0.129	0.021	0.041
	rs167396	GSN*	9	0.00583631							
5	rs1482548×	INHBA*	7	0.007007	2.95E-10	0.0064	0.01	0.164	0.129	0.015	0.038
	rs12894119	NIN*	14	0.00867969							
6	rs9550406×	MTUS2*	13	0.00543688	1.49E-09	0.0324	0.01	0.164	0.129	0.010	0.034
	rs6471951	RLBP1L1	8	0.00604041							
7	rs211953×	CXADR	21	0.000478713	3.03E-10	0.0066	0.01	0.164	0.129	0.024	0.031
	rs4881147	PITRM1*	10	0.0015086							

The Bonferroni corrected p-values (< 0.05) and R² of the SNP*SNP interaction term are shown in bold.

^a Age+Gender: Percent of variance in T-tau/A β ₄₂ level explained by age, gender.

^b Dx: Percent of variance in T-tau/A β ₄₂ level explained by diagnosis after accounting for age, gender.

^c APOE: Percent of additional variance in T-tau/A β ₄₂ level explained by the APOE genotype after accounting for age, gender and diagnosis.

^d SNP1+SNP2: Percent of additional variance in T-tau/A β ₄₂ level explained by the combined main effect of SNP1 and SNP2 after accounting for age, gender, diagnosis, and the APOE genotype.

^e SNP1*SNP2: Percent of additional variance in T-tau/A β ₄₂ level explained by the interaction effect of SNP1 and SNP2 after accounting for age, gender, diagnosis, APOE genotype, SNP1 and SNP2.

* Nearest gene proximal to the SNP.

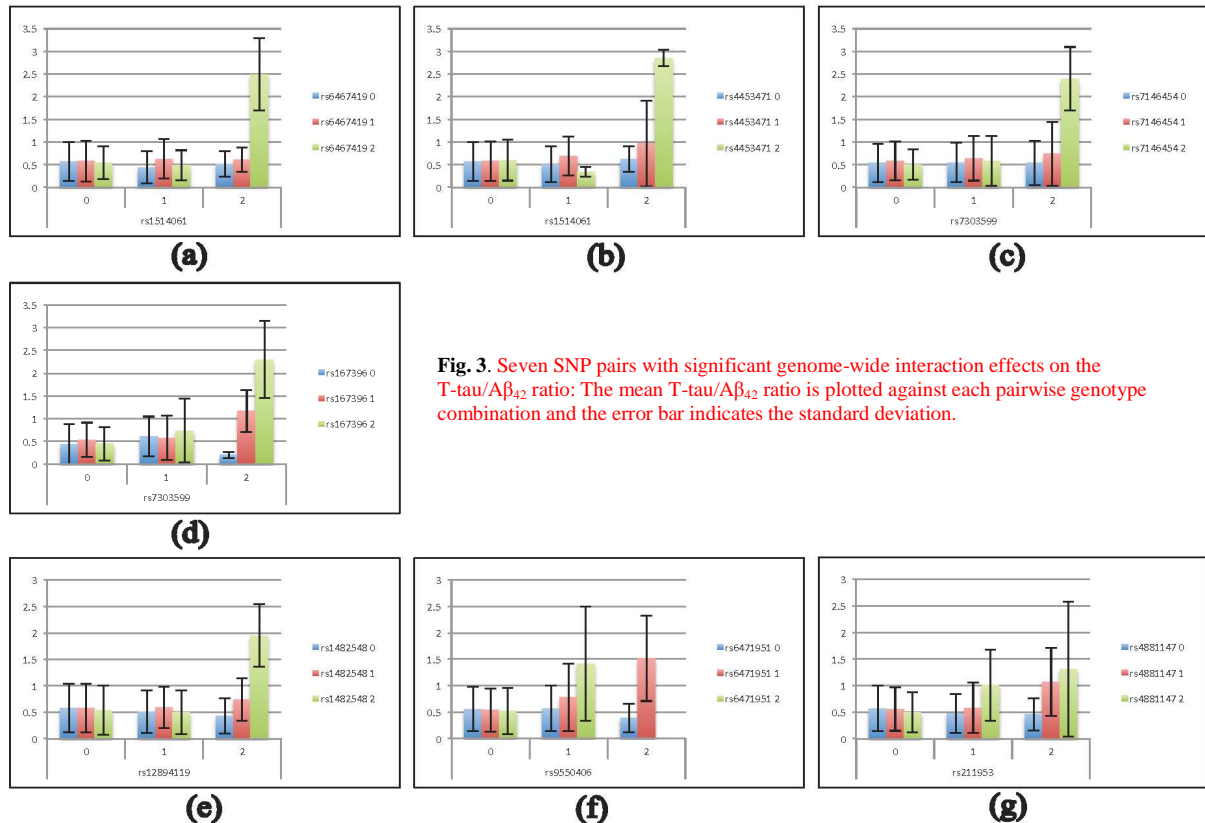


Fig. 3. Seven SNP pairs with significant genome-wide interaction effects on the T-tau/A β_{42} ratio: The mean T-tau/A β_{42} ratio is plotted against each pairwise genotype combination and the error bar indicates the standard deviation.

The protein encoded by the *INHBA* gene has been linked to neuroprotection via preventing neurons from mitochondrial dysfunction, a major cause of excitotoxicity. The corresponding process, providing protection against ischemic brain damage, could be altered in AD, or aging-related neurodegenerative conditions (Lau et al., 2015). The *NIN* gene encodes ninein (*GSK3B* interacting protein), and variants of *GSK3B* have been shown to be linked with AD and interacted with the *APOE* genotype (Izzo et al., 2013). The *MTUS2* gene encodes microtubule associated tumor suppressor candidate 2, also known as cardiac zipper protein or CAZIP. CAZIP has been shown to play a role in the development and function of the heart and nervous system in vertebrates (Du Puy et al., 2009). *PITRM1* is responsible for significant A β degradation, and the impairment of its activity results in A β accumulation (Brunetti et al., 2016). The possible mechanisms behind *INHBA-NIN*, *MTUS2-RLBP1L1*, and *CXADR-PITRM* interactions warrant further investigation.

In summary, some of the genes identified in our GWAS and GWIS have shown interesting associations with tauopathies and/or amyloid pathology related to AD from prior knowledge of current literatures, such as *APOE*, *APOC1*, *TOMM40*, *LRP6*, *S100B*, *DLG2*, *CNTNAP5*, *PLXNA4*, *CDH13*, *ADIPOR2*, *ADSSL1*, *GSN*, and *PITRM* genes (see Supplementary Tables s4a and s4b). Supplementary Tables s4a and s4b showed that these 13 genes were reported in previous genomic, cell culture, mouse model and biomarker studies, and shown to be significantly associated to CSF A β_{42} , CSF T-tau or other AD endo-phenotypes. However, in this work, only *APOE*, *APOC1*, *TOMM40* genes showed significant associations to the CSF A β_{42} , T-tau and T-tau/A β_{42} levels, other genes were not identified by GWAS and GWIS of A β_{42}

alone or T-tau alone (Supplementary Table s2 and Table s3). This indicates that, when CSF A β_{42} alone and T-tau alone show less power for detecting the risk variants, the T-tau/A β_{42} ratio has the potential to serve as a more powerful quantitative trait to identify significant variants. In addition, our study also revealed numerous SNPs and SNP-SNP pairs that had not yet been associated with AD pathology, which warrant further investigation or replication in future studies.

5. Conclusions

Aimed at studying a major AD biomarker as phenotype, we performed GWAS and GWIS to detect the main genetic effects as well as SNP-SNP interaction effects on the CSF T-tau/A β_{42} ratio. The single-marker analysis replicated the *APOE*, *APOC1* and *TOMM40* genes, which are previously confirmed AD risk genes. We also identified 14 additional loci within or proximate to *LRP6*, *S100B*, *DLG2*, *CNTNAP5*, *B3GALT2*, *FBP1*, *ITGA8*, *ATP5F1*, *LPAR3*, *DAPK2*, *DBX1*, *AADACL1*, *SGIP1*, and *ARHGAP28*. The two-marker interaction analysis identified a number of novel interaction findings, which showed strong associations with the T-tau/A β_{42} ratio. These were interactions between *PLXNA4* and *PLXNA4*, between *PLXNA4* and *CDH13*, between *ADIPOR2* and *ADSSL1*, between *ADIPOR2* and *GSN*, between *INHBA* and *NIN*, between *MTUS2* and *RLBP1L1*, and between *CXADR* and *PITRM1*. The effects of SNP-SNP interactions showed high-level statistical significance, while the corresponding single-marker effects were marginal. SNP-SNP interaction effects may help address part of “miss heritability”.

Our genome-wide association study and interaction study have the following strengths. (1) Continuous quantitative trait

T-tau/ $A\beta_{42}$ can not only gain higher statistical power, but also contribute to detecting potential risk variants related to T-tau and/or $A\beta_{42}$ at the same time. (2) Five values (1-5) indicating CN, SMC, EMCI, LMCI and AD respectively, provide a rank ordered spectrum of the AD progression. (3) In this study, both GWAS and GWIS consider age, gender, and clinical diagnosis as covariates. In the post hoc linear regression analysis we included confounding factors *APOE* $\epsilon 4$ allele (rs429358) on top of the above three covariates, and so provided more accurate estimate of the interaction effects on CSF T-tau/ $A\beta_{42}$ ratio.

The limitations of our study are as follows: (1) We examined 22 million SNP-SNP pairs and conducted an exhaust test among the SNPs. More effective and efficient strategies remain to be developed. (2) To control for potential false positives of the GWIS findings, we used two methods. One is the Bonferroni method, which corrects for multiple comparison by using a threshold of α/n and is well-known to be a conservative approach. Another method used in the work is the cell-size criterion, which excludes rare genotype combinations to avoid potential false positives. In this work, we set $\alpha=0.05$ and $n=21,717,345$ for Bonferroni correction; and for the cell-size criterion, all the cell sizes in the 3-by-3 contingency table are required to be either more than 5 or equal to 0. There are 307 pairs SNPs passed the first threshold, and subsequently only 7 pairs among 307 pairs passed the second threshold for further study. Although these are relatively stringent criteria for controlling false positives, future replication studies are required to confirm the identified interaction signals. (3) We performed the GWAS and GWIS of CSF T-tau/ $A\beta_{42}$ ratio using data-driven method. Future studies could utilize prior biological knowledge, such as biological networks, pathways databases, special tissues and other functional annotation data, to enhance statistical power and improve biological interpretability. (4) Future studies are necessary to replicate and validate the findings in independent datasets, and to uncover potential mechanisms underlying tagged by the identified SNPs and genes in our study.

Acknowledgments

Supported in part by grants from National Natural Science Foundation of China (81301297), National Key Scientific Instrument and Equipment Development Projects of China (2012YQ04014001, 2012YQ04014010), and Fundamental

Research Funds for the Central Universities (HEUCF160412); and by NIH R01 EB022574, R01 LM011360, U01 AG024904, RC2 AG036535, R01 AG19771, P30 AG10133, UL1 TR001108, NSF IIS-1117335, DOD W81XWH-14-2-0151, and NCAA 14132004 at IU.

Data collection and sharing for this project was funded by the Alzheimer's Disease Neuroimaging Initiative (ADNI) (National Institutes of Health Grant U01 AG024904) and DOD ADNI (Department of Defense award number W81XWH-12-2-0012). ADNI is funded by the National Institute on Aging, the National Institute of Biomedical Imaging and Bioengineering, and through generous contributions from the following: AbbVie, Alzheimer's Association; Alzheimer's Drug Discovery Foundation; Araclon Biotech; BioClinica, Inc.; Biogen; Bristol-Myers Squibb Company; CereSpir, Inc.; Cogstate; Eisai Inc.; Elan Pharmaceuticals, Inc.; Eli Lilly and Company; EuroImmun; F. Hoffmann-La Roche Ltd and its affiliated company Genentech, Inc.; Fujirebio; GE Healthcare; IXICO Ltd.; Janssen Alzheimer Immunotherapy Research & Development, LLC.; Johnson & Johnson Pharmaceutical Research & Development LLC.; Medpace, Inc.; Merck & Co., Inc.; Meso Scale Diagnostics, LLC.; NeuroRx Research; Neurotrack Technologies; Novartis Pharmaceuticals Corporation; Pfizer Inc.; Piramal Imaging; Servier; Takeda Pharmaceutical Company; and Transition Therapeutics. The Canadian Institutes of Health Research is providing funds to support ADNI clinical sites in Canada. Private sector contributions are facilitated by the Foundation for the National Institutes of Health (www.fnih.org). The grantee organization is the Northern California Institute for Research and Education, and the study is coordinated by the Alzheimer's Therapeutic Research Institute at the University of Southern California. ADNI data are disseminated by the Laboratory for Neuro Imaging at the University of Southern California.

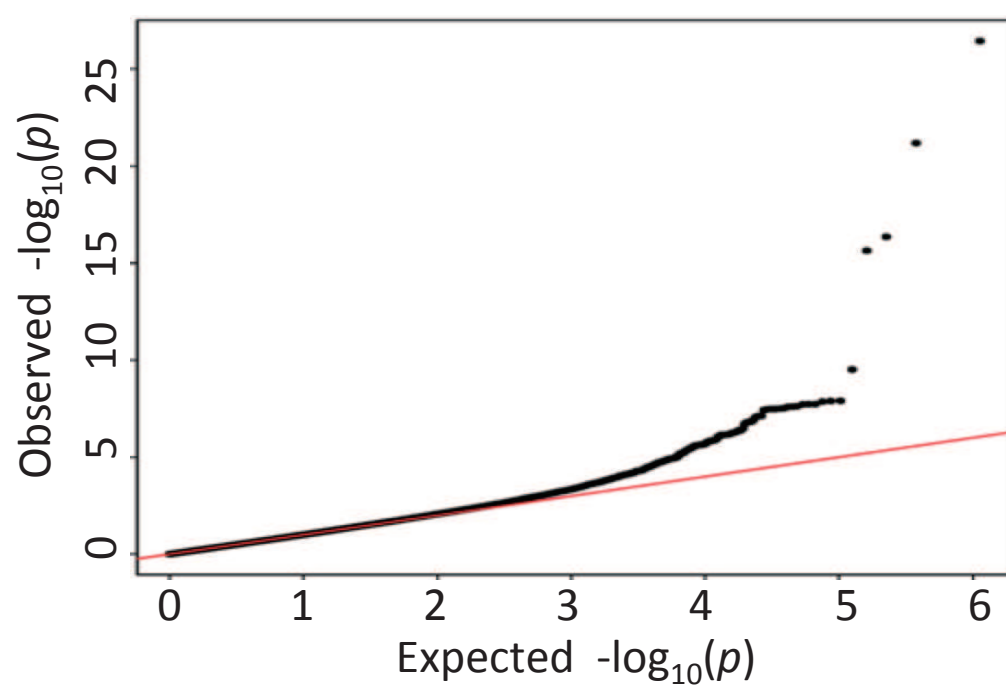
Disclosure Statement

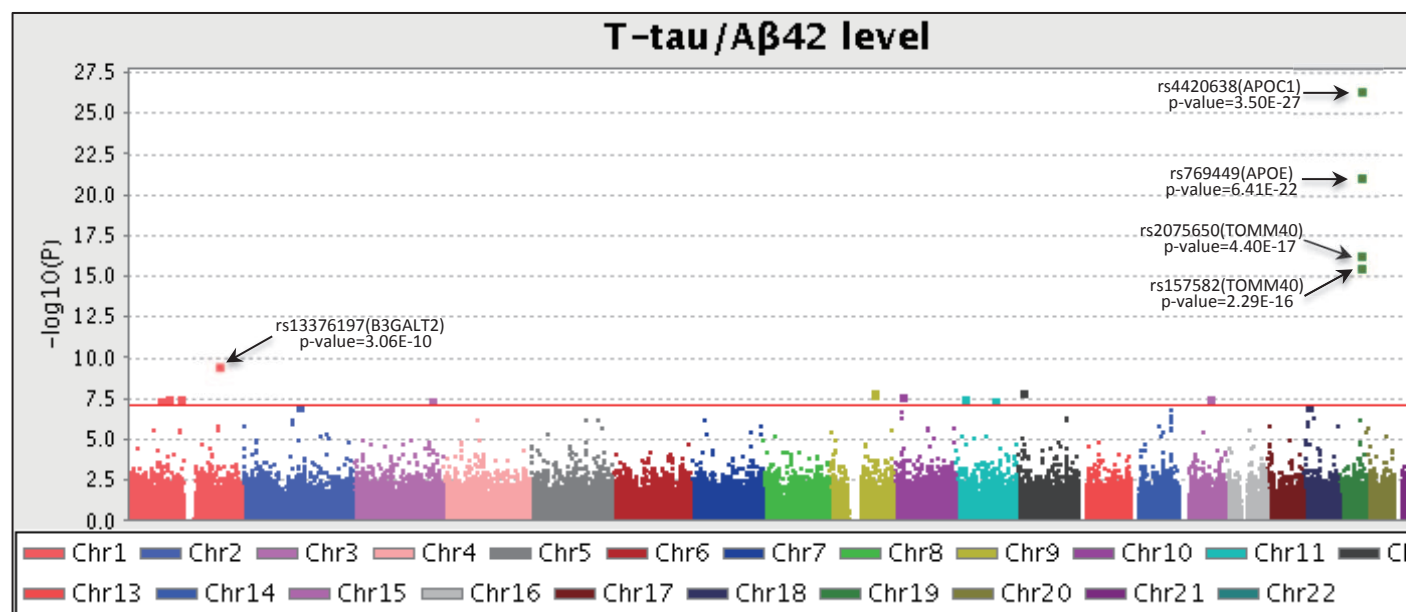
The authors have no actual or potential conflicts of interest including any financial, personal, or other relationships with other people or organizations that could inappropriately influence (bias) our work.

References

- Akiyama, H., Ikeda, K., Kondo, H., Kato, M., & McGeer, P. L. (1993). Microglia express the type 2 plasminogen activator inhibitor in the brain of control subjects and patients with Alzheimer's disease. *Neurosci Lett*, 164(1-2), 233-235.
- Becker, T., Herold, C., Meesters, C., Mattheisen, M., & Baur, M. P. (2011). Significance levels in genome-wide interaction analysis (GWIA). *Ann Hum Genet*, 75(1), 29-35. doi:10.1111/j.1469-1809.2010.00610.x
- Blennow, K., & Hampel, H. (2003). CSF markers for incipient Alzheimer's disease. *Lancet Neurol*, 2(10), 605-613.
- Brunetti, D., Torsvik, J., Dallabona, C., Teixeira, P., Sztromwasser, P., Fernandez-Vizarra, E., . . . Bindoff, L. A. (2016). Defective P1TRM1 mitochondrial peptidase is associated with Abeta amyloidotic neurodegeneration. *EMBO Mol Med*, 8(3), 176-190. doi:10.15252/emmm.201505894
- Chan, K. H., Lam, K. S., Cheng, O. Y., Kwan, J. S., Ho, P. W., Cheng, K. K., . . . Xu, A. (2012). Adiponectin is protective against oxidative stress induced cytotoxicity in amyloid-beta neurotoxicity. *PLoS One*, 7(12), e52354. doi:10.1371/journal.pone.0052354
- Deng, R., Hao, J., Han, W., Ni, Y., Huang, X., & Hu, Q. (2015). Gelsolin regulates proliferation, apoptosis, migration and invasion in human oral carcinoma cells. *Oncol Lett*, 9(5), 2129-2134. doi:10.3892/ol.2015.3002
- Dickerson, B. C., Wolk, D. A., & Alzheimer's Disease Neuroimaging, I. (2013). Biomarker-based prediction of progression in MCI: Comparison of AD signature and hippocampal volume with spinal fluid amyloid-beta and tau. *Front Aging Neurosci*, 5, 55. doi:10.3389/fnagi.2013.00055
- Du Puy, L., Beqqali, A., Monshouer-Kloots, J., Haagsman, H. P., Roelen, B. A., & Passier, R. (2009). CAZIP, a novel protein expressed in the developing heart and nervous system. *Dev Dyn*, 238(11), 2903-2911. doi:10.1002/dvdy.22107
- Fagan, A. M., Mintun, M. A., Mach, R. H., Lee, S. Y., Dence, C. S., Shah, A.

- R., . . . Holtzman, D. M. (2006). Inverse relation between in vivo amyloid imaging load and cerebrospinal fluid Abeta42 in humans. *Ann Neurol*, 59(3), 512-519. doi:10.1002/ana.20730
- Fagan, A. M., Roe, C. M., Xiong, C., Mintun, M. A., Morris, J. C., & Holtzman, D. M. (2007). Cerebrospinal fluid tau/beta-amyloid(42) ratio as a predictor of cognitive decline in nondemented older adults. *Arch Neurol*, 64(3), 343-349. doi:10.1001/archneur.64.3.noc60123
- Goudey, B., Rawlinson, D., Wang, Q., Shi, F., Ferra, H., Campbell, R. M., . . . Kowalczyk, A. (2013). GWIS--model-free, fast and exhaustive search for epistatic interactions in case-control GWAS. *BMC Genomics*, 14 Suppl 3, S10. doi:10.1186/1471-2164-14-S3-S10
- Hempel, H., Blennow, K., Shaw, L. M., Hoessler, Y. C., Zetterberg, H., & Trojanowski, J. Q. (2010). Total and phosphorylated tau protein as biological markers of Alzheimer's disease. *Exp Gerontol*, 45(1), 30-40. doi:10.1016/j.exger.2009.10.010
- Herold, C., Steffens, M., Brockschmidt, F. F., Baur, M. P., & Becker, T. (2009). INTERSNP: genome-wide interaction analysis guided by a priori information. *Bioinformatics*, 25(24), 3275-3281. doi:10.1093/bioinformatics/btp596
- Hohman, T. J., Koran, M. E., Thornton-Wells, T. A., & Alzheimer's Disease Neuroimaging, I. (2014). Genetic modification of the relationship between phosphorylated tau and neurodegeneration. *Alzheimers Dement*, 10(6), 637-645 e631. doi:10.1016/j.jalz.2013.12.022
- Hondius, D. C., van Nierop, P., Li, K. W., Hoozemans, J. J., van der Schors, R. C., van Haastert, E. S., . . . Smit, A. B. (2016). Profiling the human hippocampal proteome at all pathologic stages of Alzheimer's disease. *Alzheimers Dement*, 12(6), 654-668. doi:10.1016/j.jalz.2015.11.002
- Izzo, G., Forlenza, O. V., Santos, B., Bertolucci, P. H., Ojopi, E. B., Gattaz, W. F., & Kerr, D. S. (2013). Single-nucleotide polymorphisms of GSK3B, GAB2 and SORL1 in late-onset Alzheimer's disease: interactions with the APOE genotype. *Clinics (Sao Paulo)*, 68(2), 277-280.
- Jagust, W. J., Landau, S. M., Shaw, L. M., Trojanowski, J. Q., Koeppe, R. A., Reiman, E. M., . . . Alzheimer's Disease Neuroimaging, I. (2009). Relationships between biomarkers in aging and dementia. *Neurology*, 73(15), 1193-1199. doi:10.1212/WNL.0b013e3181bc010c
- Jun, G., Asai, H., Zeldich, E., Drapeau, E., Chen, C., Chung, J., . . . Farrer, L. A. (2014). PLXNA4 is associated with Alzheimer disease and modulates tau phosphorylation. *Ann Neurol*, 76(3), 379-392. doi:10.1002/ana.24219
- Kabogo, D., Rauw, G., Amritraj, A., Baker, G., & Kar, S. (2010). ss-amyloid-related peptides potentiate K+-evoked glutamate release from adult rat hippocampal slices. *Neurobiol Aging*, 31(7), 1164-1172. doi:10.1016/j.neurobiolaging.2008.08.009
- Kohannim, O., Hibar, D. P., Stein, J. L., Jahanshad, N., Hua, X., Rajagopalan, P., . . . Alzheimer's Disease Neuroimaging, I. (2012). Discovery and Replication of Gene Influences on Brain Structure Using LASSO Regression. *Front Neurosci*, 6, 115. doi:10.3389/fnins.2012.00115
- Lau, D., Bengtson, C. P., Buchthal, B., & Bading, H. (2015). BDNF Reduces Toxic Extrasynaptic NMDA Receptor Signaling via Synaptic NMDA Receptors and Nuclear-Calcium-Induced Transcription of inhba/Activin A. *Cell Rep*, 12(8), 1353-1366. doi:10.1016/j.celrep.2015.07.038
- Li, J., Zhang, Q., Chen, F., Yan, J., Kim, S., Wang, L., . . . Shen, L. (2015). Genetic Interactions Explain Variance in Cingulate Amyloid Burden: An AV-45 PET Genome-Wide Association and Interaction Study in the ADNI Cohort. *Biomed Res Int*, 2015, 647389. doi:10.1155/2015/647389
- Li, Q. S., Parrado, A. R., Samtani, M. N., Narayan, V. A., & Alzheimer's Disease Neuroimaging, I. (2015). Variations in the FRA10A1 Fragile Site and 15q21 Are Associated with Cerebrospinal Fluid Abeta1-42 Level. *PLoS One*, 10(8), e0134000. doi:10.1371/journal.pone.0134000
- Liu, C. C., Tsai, C. W., Deak, F., Rogers, J., Penuliar, M., Sung, Y. M., . . . Bu, G. (2014). Deficiency in LRP6-mediated Wnt signaling contributes to synaptic abnormalities and amyloid pathology in Alzheimer's disease. *Neuron*, 84(1), 63-77. doi:10.1016/j.neuron.2014.08.048
- Mukaetova-Ladinska, E. B., Abdel-All, Z., Mugica, E. S., Li, M., Craggs, L. J., Oakley, A. E., . . . Kalaria, R. N. (2015). Tau proteins in the temporal and frontal cortices in patients with vascular dementia. *J Neuropathol Exp Neurol*, 74(2), 148-157. doi:10.1097/NEN.0000000000000157
- Pan, C., Korff, A., Galasko, D., Ginghina, C., Peskind, E., Li, G., . . . Zhang, J. (2015). Diagnostic Values of Cerebrospinal Fluid T-Tau and Abeta(4)(2) using Meso Scale Discovery Assays for Alzheimer's Disease. *J Alzheimers Dis*, 45(3), 709-719. doi:10.3233/JAD-143099
- Peskind, E. R., Griffin, W. S., Akama, K. T., Raskind, M. A., & Van Eldik, L. J. (2001). Cerebrospinal fluid S100B is elevated in the earlier stages of Alzheimer's disease. *Neurochem Int*, 39(5-6), 409-413. doi:10.3233/JAD-143099
- Petzold, A., Keir, G., Lim, D., Smith, M., & Thompson, E. J. (2003). Cerebrospinal fluid (CSF) and serum S100B: release and wash-out pattern. *Brain Res Bull*, 61(3), 281-285.
- Pharoah, P. D., Tsai, Y. Y., Ramus, S. J., Phelan, C. M., Goode, E. L., Lawrenson, K., . . . Sellers, T. A. (2013). GWAS meta-analysis and replication identifies three new susceptibility loci for ovarian cancer. *Nat Genet*, 45(4), 362-370, 370e361-362. doi:10.1038/ng.2564
- Price, A. L., Patterson, N. J., Plenge, R. M., Weinblatt, M. E., Shadick, N. A., & Reich, D. (2006). Principal components analysis corrects for stratification in genome-wide association studies. *Nat Genet*, 38(8), 904-909. doi:10.1038/ng1847
- Pritchard, J. K., Stephens, M., & Donnelly, P. (2000). Inference of population structure using multilocus genotype data. *Genetics*, 155(2), 945-959.
- Purcell, S., Neale, B., Todd-Brown, K., Thomas, L., Ferreira, M. A., Bender, D., . . . Sham, P. C. (2007). PLINK: a tool set for whole-genome association and population-based linkage analyses. *Am J Hum Genet*, 81(3), 559-575. doi:10.1086/519795
- Rosenthal, S. L., Wang, X., Demirci, F. Y., Barmada, M. M., Ganguli, M., Lopez, O. L., & Kamboh, M. I. (2012). Beta-amyloid toxicity modifier genes and the risk of Alzheimer's disease. *Am J Neurodegener Dis*, 1(2), 191-198.
- Saykin, A. J., Shen, L., Foroud, T. M., Potkin, S. G., Swaminathan, S., Kim, S., . . . Weiner, M. W. (2010). Alzheimer's Disease Neuroimaging Initiative biomarkers as quantitative phenotypes: Genetics core aims, progress, and plans. *Alzheimers Dement*, 6(3), 265-273. doi:10.1016/j.jalz.2010.03.013
- Schott, J. M., Crutch, S. J., Carrasquillo, M. M., Uphill, J., Shakespeare, T. J., Ryan, N. S., . . . Mead, S. (2016). Genetic risk factors for the posterior cortical atrophy variant of Alzheimer's disease. *Alzheimers Dement*. doi:10.1016/j.jalz.2016.01.010
- Shaw, L. M., Vanderstichele, H., Knapik-Czajka, M., Clark, C. M., Aisen, P. S., Petersen, R. C., . . . Alzheimer's Disease Neuroimaging, I. (2009). Cerebrospinal fluid biomarker signature in Alzheimer's disease neuroimaging initiative subjects. *Ann Neurol*, 65(4), 403-413. doi:10.1002/ana.21610
- Shen, L., Kim, S., Risacher, S. L., Nho, K., Swaminathan, S., West, J. D., . . . Alzheimer's Disease Neuroimaging, I. (2010). Whole genome association study of brain-wide imaging phenotypes for identifying quantitative trait loci in MCI and AD: A study of the ADNI cohort. *Neuroimage*, 53(3), 1051-1063. doi:10.1016/j.neuroimage.2010.01.042
- Shen, L., Thompson, P. M., Potkin, S. G., Bertram, L., Farrer, L. A., Foroud, T. M., . . . Alzheimer's Disease Neuroimaging, I. (2014). Genetic analysis of quantitative phenotypes in AD and MCI: imaging, cognition and biomarkers. *Brain Imaging Behav*, 8(2), 183-207. doi:10.1007/s11682-013-9262-z
- Wan, Z., Mah, D., Simtchouk, S., Klegeris, A., & Little, J. P. (2014). Globular adiponectin induces a pro-inflammatory response in human astrocytic cells. *Biochem Biophys Res Commun*, 446(1), 37-42. doi:10.1016/j.bbrc.2014.02.077
- Wang, H., Sun, F. R., Tan, L., Wang, H. F., Zhang, W., Wang, Z. X., . . . Tan, L. (2016). Association study of the PLXNA4 gene with the risk of Alzheimer's disease. *Ann Transl Med*, 4(6), 108. doi:10.21037/atm.2016.03.23
- Yang, W., Chauhan, A., Mehta, S., Mehta, P., Gu, F., & Chauhan, V. (2014). Trichostatin A increases the levels of plasma gelsolin and amyloid beta-protein in a transgenic mouse model of Alzheimer's disease. *Life Sci*, 99(1-2), 31-36. doi:10.1016/j.lfs.2014.01.064





Highlights

- SNP-SNP interaction effects may help address part of “miss heritability”.
- GWAS and GWIS of T-tau/ $A\beta_{42}$ ratio were performed on the landmark ADNI database.
- This is the first GWIS on the quantitative trait of the T-tau/ $A\beta_{42}$ ratio.
- The interaction results had marginal main effects but explained relatively high level T-tau/ $A\beta_{42}$ variance.